Indoor Air 2005; 15: 367–380
www.blackwellpublishing.com/ina
Printed in Singapore. All rights reserved

INDOOR AIR
doi:10.1111/j.1600-0668.2005.00383.x

Removal of contaminants released from room surfaces by displacement and mixing ventilation: modeling and validation

Abstract This paper presents the experimental and numerical modeling of contaminant dispersion in a full-scale environmental chamber with different room air distribution systems. For the experimental modeling, an area source with uniform emissions of a hypothetical contaminant (SF_6) from the entire floor surface is designed and constructed. Two different types of ventilation are studied: displacement and mixing ventilation. A computer model for predicting the contaminant dispersion in indoor spaces was validated with experimental data. The validated model is used to study the effects of airflow and the area-source location on contaminant dispersion. Results show that the global airflow pattern has a strong impact on the distribution of the contaminants. In general, the personal exposure could be estimated by analyzing the relative source positions in the airflow pattern. Accordingly, the location of an exhaust diffuser may not greatly affect the airflow pattern, but can significantly affect the exposure level in the room.

G. He[1], X. Yang[2], J. Srebric[3]
[1]Division of Marine Geology and Geophysics, Rosenstiel School of Marine and Atmospheric Science, University of Miami, Miami, FL, USA, [2]Department of Civil, Architectural, and Environmental Engineering, University of Miami, Coral Gables, FL, USA, [3]Department of Architectural Engineering, The Pennsylvania State University, University Park, PA, USA

Key words: Area Source; Indoor Air Quality; Validation; Displacement Ventilation; Mixing Ventilation.

Xudong Yang
Department of Civil Architectural, and Environmental Engineering
University of Miami
Coral Gables, FL 33124-0630, USA
Tel.: +1 305 284 3456
Fax: +1 305 284 3492
e-mail: xudongy@miami.edu

Received for review 15 March 2004. Accepted for publication 20 June 2005.

Practical Implications
When designing ventilation in addition to bringing fresh air to occupants, it is important to consider the removal of contaminants released in the off-gassing of building materials. Typical indoor off-gassing examples are emissions of volatile organic compounds from building enclosure surfaces such as flooring and painted walls. In this study, we conducted experimental and numerical modeling of different area sources in a mock-up office setup, with displacement or mixing ventilation. Displacement ventilation was as successful as mixing ventilation in removing the contaminant source from the floor area. Actually, the most important consideration in the removal of these contaminants is the relative position of the area source to the main airflow pattern and the occupied zone.

Introduction

Heating, ventilating and air-conditioning (HVAC) systems need to be properly designed to provide thermal comfort as well as to remove indoor-generated contaminants. For indoor contaminant control, ventilation provides sufficient amount of outdoor air to enable effective air distribution in the room. An effective air distribution system requires proper placement of supply and exhaust diffusers with respect to the room configuration, source distribution and thermal conditions. Our study examined contaminant removal by two of the currently most popular air distribution systems: displacement and mixing ventilation.

In ventilated spaces, the airflow pattern created by the air distribution system is crucial for contaminant distribution. The main factors that affect the airflow pattern and contaminant distribution are type and location of supply and exhaust diffuser(s), location of heat sources and their intensity, human activities, room partitioning, and vertical airflow along windows and walls with surface temperatures different from the local room air temperatures. In a displacement ventilation system, when the contaminant sources are associated with heat sources, the plume is a favorable flow pattern to transport the contaminants from the lower to the upper part of the room. However, for the passive contaminant sources (sources not associated with heat

release) located at lower level, the occupant plume may bring the contaminants from the lower level to the breathing zone and thus make the air quality worse at the breathing zone (Brohus and Nielsen, 1996).

For the contaminant dispersion in a ventilated space, both the type and location of pollutant sources should be taken into consideration. Nowadays, most studies use point sources (Hagström et al., 2002; Srebric and Chen, 2002; Yuan et al., 1999) or a small-area source (Cheong et al., 2003; Hagström et al., 1999). Brohus (1997) considered a large planar contaminant source scenario in a ventilated room and simulated the contaminant dispersion using computational fluid dynamics (CFD). The simulation results were not compared with the experimental measurements. Based on the current state-of-the-art, our study started with experiments.

This paper presents both the experimental and numerical results of air and contaminant dispersion in a mock-up office setting with different air distribution methods. Different air-supply diffusers were used to create displacement and mixing ventilation. A passive area source with constant emissions of a tracer gas (SF_6) from the whole floor surface was designed to simulate a realistic area source such as flooring. The objectives of experimental measurements were to collect data for evaluating the effects of different airflow patterns on ventilation effectiveness, and to validate the CFD model. The validated CFD model was further used to study and quantify contaminant concentrations under additional scenarios of air diffuser layouts and contaminant sources. This benchmark validation saved time and costs required by the experiments, while reliable additional data could be obtained from the numerical simulations. The additional data enabled general recommendations for different air distribution systems in the removal of indoor contaminants released from an area source.

Experimental measurements

The test chamber and air distribution systems

The experiments were conducted using a full-scale environmental chamber ($5.16 \times 3.65 \times 2.26$ m) shown in Figure 1. The east wall with window separated the test room from the neighboring climate room (not shown), which was designed to provide different climatic conditions for the test room.

Four different air distribution systems using a displacement, square, slot, and grille diffuser, respectively, were tested (Figure 2). Displacement diffuser represented displacement ventilation, while square, slot, and grille diffuser created mixing ventilation. Figure 1 shows supply and exhaust diffuser locations for all four air distribution systems. The displacement diffuser was placed on the floor against the west wall, and the exhaust in the middle of the ceiling. All the other three supply diffusers had the same exhaust at the lower part of the west wall. Each of the experiments had only one supply and one exhaust diffuser active, while the other ones were tightly sealed. Based on the smoke visualization tests, the jet from the grille diffuser showed an angle of approximately 18° upward and 7° toward the south wall. For the slot diffuser, the jet was discharged horizontally toward the west wall. For the square diffuser, the supply air was discharged horizontally in all directions.

The HVAC system, located outside of the room, supplied air at controlled flow rate, temperature, and humidity to the room through each of the diffusers. The test room also included two tables, two human simulators, two computers, four overhead fluorescent lights, and two boxes simulating two pieces of furniture. Table 1 lists the internal heat sources and their location coordinates, sizes, and heat flow rates.

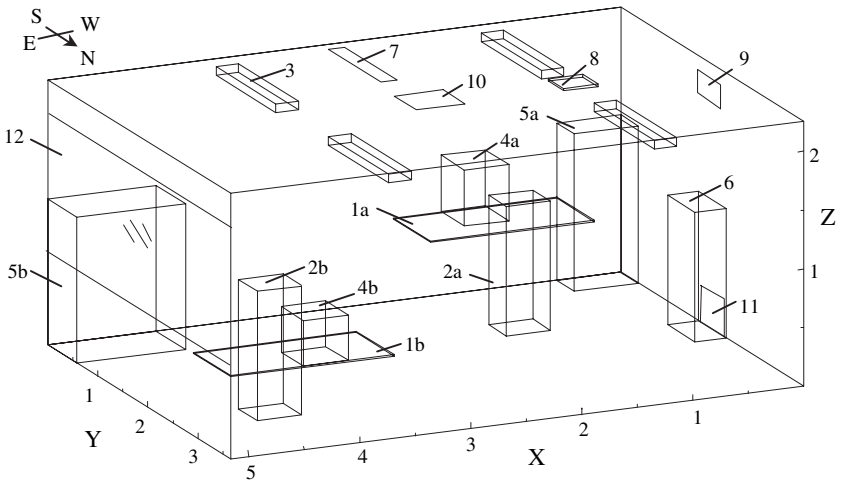

Fig. 1 Configuration of the mockup office and placement of ventilation diffusers (1, tables; 2, person simulators; 3, lamps; 4, computers; 5, cabinets; 6, displacement diffuser; 7, slot diffuser; 8, square diffuser; 9, grill diffuser; 10, ceiling exhaust for displacement ventilation; 11, wall exhaust for mixing ventilation; 12, window)

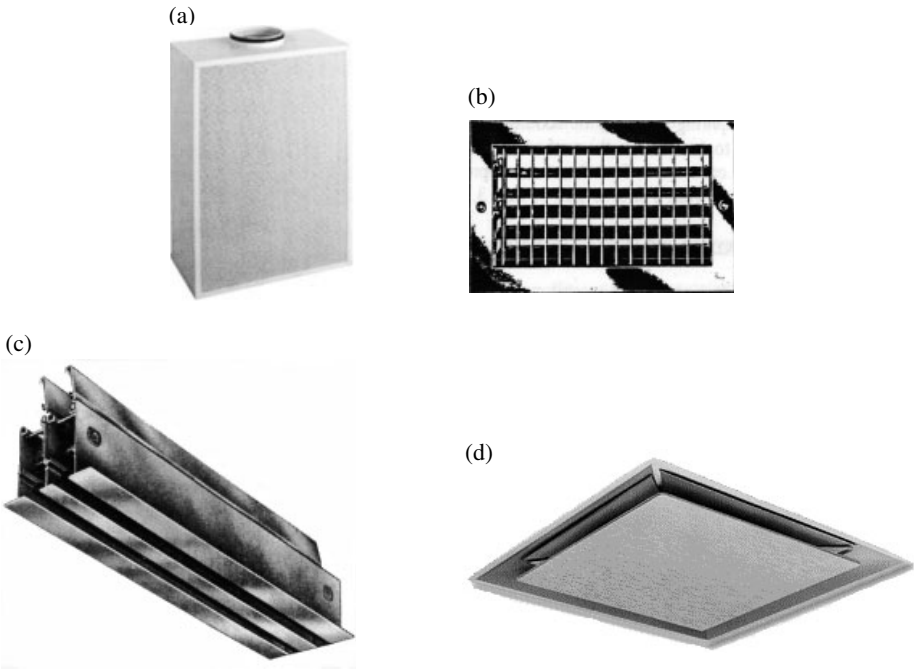

Fig. 2 Air-supply diffusers used in this study: (a) displacement, (b) grille, (c) slot, and (d) square diffuser

Setup of the area contaminant source

Laboratory representation of a uniform area source is very challenging because of the source size and constant emission rate requirements. Figure 3 shows the raised floor structure used in our experiment to simulate an area source with uniform and constant emission rate of a tracer gas SF_6. A 1 cm thick wood board was drilled with many small holes and was covered with two layers of highly permeable foam padding. The source, 1.01% SF_6, was introduced into the tubing net [Polytetrafluorethylene (PTFE), inert to chemicals], laid across the floor plenum. Small holes were drilled along the tubing to ensure uniform concentration of SF_6 in the plenum. SF_6 was diffused into the room through the holes on the perforated board and the foam padding. A total of 10 tubes were deployed on the floor surface, and eight small fans were used to further mix the SF_6 in the floor plenum. The flow rate of SF_6 was controlled by a rotameter. The emission rate was calculated from the SF_6 injection rate and the effective emission area.

Table 1 Room configurations and internal heat sources (same for all ventilation cases other than specified)

	Location (m)			Size (m)			
Name	*X*	*Y*	*Z*	ΔX	ΔY	ΔZ	Total heat (*w*)
Comp1 (4a)	1.22	0	0.711	0.4	0.47	0.48	87.6
Comp2 (4b)	4.1	3.2	0.711	0.4	0.45	0.389	74.4
Table 1 (1a)	0.58	0	0.70	1.47	0.75	0.011	–
Table 2 (1b)	3.69	2.9	0.70	1.47	0.75	0.011	–
Person1 (2a)	1.22	0.95	0	0.4	0.35	1.1	66
Person2 (2b)	4.1	2.35	0	0.4	0.37	1.1	43.2
Cabinet1 (5a)	0	0	0	0.58	0.35	1.34	–
Cabinet2 (5b)	4.18	0	0	0.98	0.58	1.24	–
Lamp1 (3)	1.1	0.1	2.15	0.2	1.2	0.07	25
Lamp2 (3)	1.1	2.35	2.15	0.2	1.2	0.07	25
Lamp3 (3)	3.49	0.1	2.15	0.2	1.2	0.07	25
Lamp4 (3)	3.49	2.35	2.15	0.2	1.2	0.07	25
Displacement diffuser[a] (6)	0	1.555	0	0.28	0.54	1.1	–
Square diffuser (8)	1.1	1.673	2.24	0.305	0.305	0.02	–
Grille diffuser (9)	0	1.68	1.95	0	0.29	0.2	–
Slot diffuser (7)	2.553	0.15	2.26	-	1.25	0.305	–
Wall exhaust (11)	0	1.596	0	0	0.457	0.317	–
Ceiling Exhaust (10)	2.33	1.61	2.26	0.44	0.44	0	–

[a]Present only in the displacement ventilation case.

The uniformity of emissions at the surface was tested by measuring the concentrations immediately above the floor without room ventilation. Concentrations at 30 spots were measured as shown by the solid circles in Figure 3. Those measurements resulted in an average SF_6 concentration of 22.03 mg/m^3 and a standard deviation of 4.65 mg/m^3. Overall, the emission was fairly uniform across the floor area because of the engineering solution for the uniform source representation with perforated tubing, permeable padding, perforated board, and small mixing fans.

Acquisition equipment and measurement locations

Distributions of velocity, temperature, and SF_6 concentration were measured in many discrete room locations. In addition, the following parameters were also measured: wall temperatures, airflow rates, supply parameters (jet discharge velocity, temperature, and

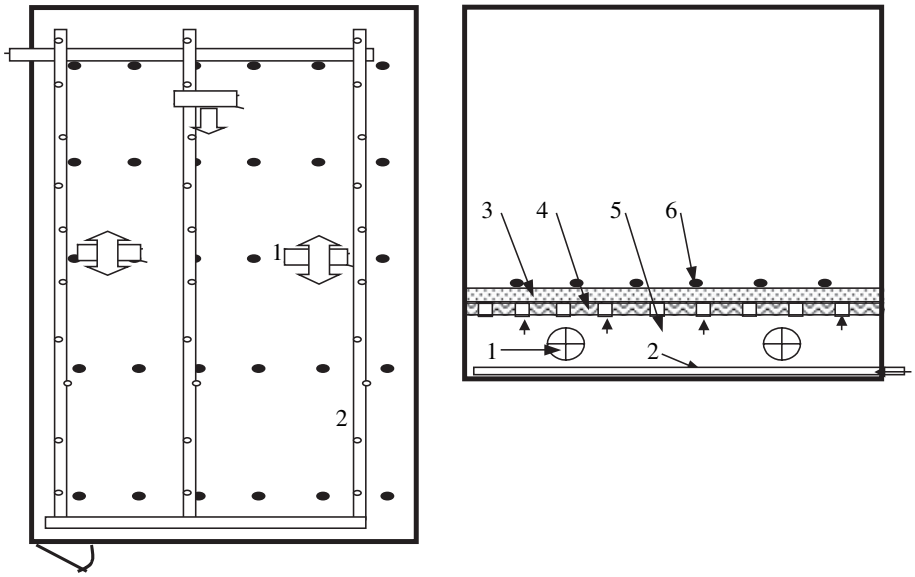

Fig. 3 Area source and measuring spots (solid circles) for emission uniformity test. 1, fans (eight small mixing fans); 2, tubing with uniformly distributed holes (10 tubes); 3, carpet pad (foam); 4, perforated wood board; 5, floor plenum; 6, measuring spots

concentration), and exhaust parameters (temperature and concentration). Therefore, the acquisition equipment includes hot-sphere anemometers, thermocouples, and a tracer gas analyzer.

Altogether, 28 hot-sphere anemometers were used to measure the temperature and velocity distributions in the room. The velocity measurement range of the anemometers was from 0.05 to 5 m/s with a repeatability of 0.01 m/s, or $\pm 2\%$ when velocity magnitude was above 0.15 m/s. When velocity magnitude was below 0.10 m/s, the anemometers were not able to measure the velocity reliably. The hot-sphere anemometer measured temperatures at a resolution of 0.3°C. Thermocouples were also used to measure the temperatures and they also had a resolution of 0.3°C. The tracer gas concentration was sampled and analyzed by a multi-gas monitor (1302 monitor; Bruel and Kjaer Instruments, Inc., Marlborough, MA, USA) and sampler (1309 sampler, Bruel and Kjaer, USA). This system has a detection threshold of 10^{-3} ppm and 1% repeatability. Four movable poles were placed in the test room, and each supported multiple hot-sphere anemometers, thermocouples, and air-sampling tubes at different heights. Eight measuring positions were selected, which were marked by a number followed by an upper case letter in Figure 4 (1A, 2A, 3A, 4A and 1B, 2B, 3B, 4B).

The wall temperatures were measured at 67 locations: 15 positions for the east, south, and north walls, each; six for the west wall; eight for the ceiling; and eight for the floor. The measurements were conducted with thermocouples and a digital infrared temperature scanner (range: −45 to 287°C, accuracy 0.1°C). In displacement ventilation, the sidewalls had an increasing temperature profile with height. In the other three cases of mixing ventilation, the sidewall temperatures tended to be uniform. Table 2 shows the measured sidewall temperatures with displacement ventilation.

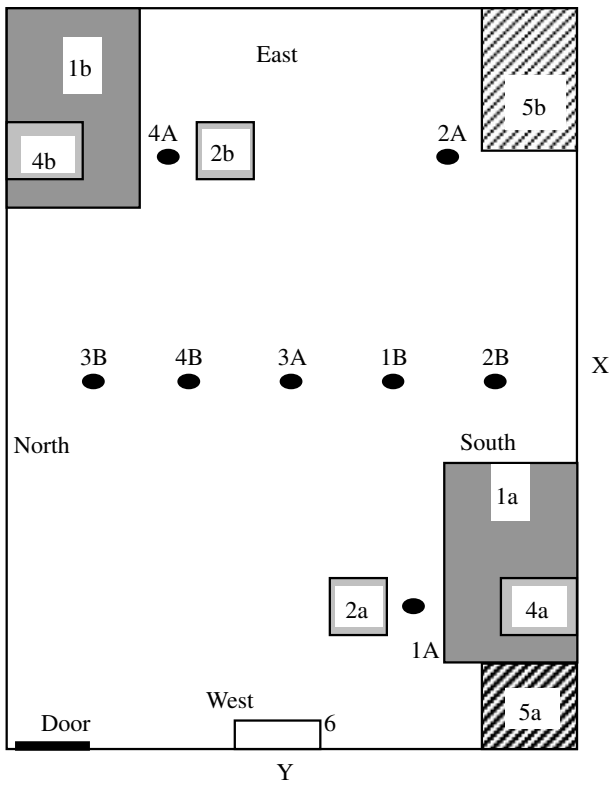

Fig. 4 Horizontal room section and measuring pole positions (1A, 2A, 3A, 4A and 1B, 2B, 3B, 4B). Sensors are attached to each pole at different heights

Table 2 Enclosure temperatures (°C) measured at the sidewalls with displacement ventilation

South wall[a] ($Y = 0.0$ m)	Z (m)	0.254	0.71	1.143	1.6	2.0
	$X = 0.86$ m	22.4	23.1	24.87	24.8	25.07
	$X = 2.58$ m	23.0	23.8	23.9	24.4	23.89
	$X = 4.3$ m	23.31	23.7	24.4	24.8	24.77
North wall[a] ($Y = 3.65$ m)	Z (m)	0.254	0.71	1.143	1.6	2.0
	$X = 0.86$ m	22.5	23.0	23.7	24.1	24.31
	$X = 2.58$ m	22.9	23.3	23.69	23.9	23.68
	$X = 4.3$ m	23.6	25.7	28.4	26.2	25.57
East wall ($X = 5.16$ m)	Z (m)	0.18	0.56	1.0	1.64	2.1
	$Y = 0.61$ m	22.91	23.5	23.73	24.27	24.7
	$Y = 1.83$ m	23.7	23.59	23.99	24.15	24.7
	$Y = 2.43$ m	23.30	23.7	24.31	24.44	25.11
West wall ($X = 0$ m)	Z (m)	0.3	0.84	1.4	1.96	–
	$Y = 0.91$	22.5	23.8	24.4	23.69	–
	$Y = 2.73$	22.4	23.4	23.8	23.6	–

[a]Highest enclosure temperatures are measured locally right above the computers: 28.5°C at $X = 1.42$ m, $Y = 0$ m, $Z = 1.25$ m; 28.4°C at $X = 4.7$ m, $Y = 3.65$ m, $Z = 1.25$ m.

The discharge velocities of the jet flow in front of the diffusers were measured by a portable handheld thermal anemometer (TA5, Airflow Technical Products, Inc., Andover, NJ, USA) with a resolution of 0.01 m/s. The data were used to determine the jet momentum from the supply diffusers.

The pressure difference between the room and surrounding environment was monitored by a digital manometer. To prevent any infiltration into the test room, a slightly positive pressure was maintained during the tests.

Test procedure

The air exchange rate was set through the automatic control system by adjusting the dampers in the supply and exhaust ducts of the HVAC system. The measurement of the ventilation rate was calibrated using the SF_6 mass balance based on the SF_6 injection rate and the measured supply and exhaust concentrations. The supply air was 100% outdoor air with a very low background concentration of SF_6 (< 0.16 mg/m^3), resulting from the unavoidable cross-contamination between the exhaust and supply air intake.

For each of the four ventilation systems, the measurements were conducted twice under steady-state conditions. Before each test, the room was initially ventilated for more than 12 h to reach a thermal steady state. Then, the tracer gas was injected and allowed to reach its own steady state (about 4 h). The measurements of temperature, velocity, and concentration distributions were conducted for four poles at their initial positions (1A, 2A, 3A, 4A; Figure 4). Wall temperatures were recorded before the four poles were moved to their final positions (1B, 2B, 3B, 4B). It took about 1–2 h for the steady state to be re-established after interruption during the pole relocation. Other necessary parameters, such as supply and return temperatures, supply and exhaust concentrations, and velocity distribution of the diffusers were measured right after the second recording of the pole data.

It took about 1 min for the multi-gas monitor to draw the sample and another minute to analyze it. While the first sample was being analyzed, the drawing of the next sample was started. Four sweeps were carried out so that four discrete samples were taken for each measuring point and the average value was used to represent the concentration at the measurement location. The velocity and the temperature that were measured by the anemometers were averaged over 2 min, containing about 700 data points. The temperatures measured by thermocouples were recorded every 10 min and the data were averaged.

CFD modeling

A CFD analysis needs to be properly verified and validated. Chen and Srebric (2002) have suggested a detailed procedure for verification and validation of indoor environment CFD analyses. In our study, a commercial CFD program (CHAM, 2000) was verified by the selection of an appropriate turbulence model, boundary conditions for supply/exhaust diffusers, temperature and contaminant sources as well as the numerical solution method.

Selection of turbulence model

To simulate indoor airflow and contaminant dispersion using the CFD technique, a proper turbulence model needs to be selected among many available models. Our study used the re-normalization group (RNG) k-ε model (Yokhot et al., 1992) accompanied by the logarithmic wall functions (Launder and Spalding, 1974). The RNG model produced good validated results for indoor airflow, temperature, and contaminant distributions in several previous studies (Srebric and Chen, 2002; Yuan et al., 1999). The previous studies focused on point-source contaminant dispersion with displacement ventilation in office settings similar to those in the present study. The only important difference is that the present study used the area source instead of the point source. Nevertheless, RNG k-ε model was expected to perform well in the present study because of the similarities with the previously published work.

Boundary conditions

To solve for the airflow field, boundary conditions for supply/exhaust diffusers, heat transfer and the contaminant source need to be properly defined. One of the important and also difficult boundaries is the supply diffuser. As simulating the detailed diffuser

geometry can be very time consuming and demands a lot of the computer capacity, simplified methods are preferred. The idea of simplification is to simulate the supply jet momentum without considering the detailed diffuser geometry. Diffuser models that follow this idea could be grouped into two categories (Fan, 1995): momentum modeling at the air-supply devices (momentum method) and momentum modeling in front of the air-supply devices (box method). The momentum method (Chen and Moser, 1991) imposes initial jet momentum as a boundary condition for CFD simulations, while the box method (Nielsen, 1989, 1997) uses the momentum downstream from the diffuser. Both approaches are commonly used and their applications depend on the diffuser type (Srebric and Chen, 2002).

Srebric and Chen (2002) studied the simulation of several diffusers including displacement, grille, slot, square ceiling, round ceiling, and vortex ceiling diffusers using both momentum and box methods. In our study, the simulation of diffusers followed the recommendations of Srebric and Chen's work: the box method was used for the slot diffuser and the momentum method for the displacement, square and grille diffusers. Table 3 gives the measured supply and return parameters for each diffuser case.

In addition to the diffuser settings, thermal boundary conditions are also crucial for simulation result accuracy. The heat was transferred mainly by convection and radiation because the test chamber had an excellent insulation and similar temperature to the surrounding environment. The radiation was not calculated in the simulation. Instead, it was taken into account indirectly by setting the wall temperatures. It is assumed that 70% of the total heat is transferred by convection.

The ventilation rate was determined by mass balance of SF_6 using the injection rate and the measured supply and exhaust concentrations. The emission rate was estimated from the injection rate and the effective emission area. In displacement ventilation, the source emission rate was 0.01912 mg/m^2 and in mixing cases, the emission rate was slightly smaller: 0.01896 mg/m^2. The difference was mainly because of the removal of the displacement diffuser from the floor in mixing cases, leaving a larger emission area.

Table 3 Supply and return parameters for the four studied ventilation systems

	Displacement diffuser	Slot diffuser	Square diffuser	Grille diffuser
Ventilation rate (m^3/s)	0.056	0.051	0.053	0.067
Inlet temperature (°C)	15.9	16.9	18.0	18.5
Exhaust temperature (°C)	24.6	22.8	26.6	24.2
Inlet concentration (mg/m^3)	0.15	0.16	0.16	0.16
Exhaust concentration (mg/m^3)	6.16	6.77	6.51	5.16

Numerical solution method

Two computer programs were used to perform the numerical calculations: a commercial CFD program (CHAM, 2000) and a noncommercial program ACCESS-IAQ (Yang and Chen, 2001). The airflow field, together with thermal distribution, was first calculated by the commercial CFD program. Then, the calculated airflow was used as an input to ACCESS-IAQ to calculate the concentration distributions. ACCESS-IAQ was developed to calculate emission/sorption of sources coupled with the computed airflow from any other CFD program. When the contaminants exert little or no influence on the airflow field, the airflow and concentration calculations were separated. The separation exhibited the advantages of faster convergence and more convenience in simulating different contaminant distributions with the same airflow field. Both programs used the finite volume method with orthogonal structured grids. Discretized airflow equations were solved with the SIMPLE algorithm (Patankar, 1980) using hybrid differencing scheme for the convection term in the CFD program. In ACCESS-IAQ, the upwind-difference scheme is used for the convection term in the concentration equation. Following the previous studies of similar room settings (Yuan et al., 1999) as well as our grid independence tests (Srebric et al., 2005), a grid size of 123,840 control volumes ($60 \times 48 \times 43$) was used for the displacement ventilation case. The other cases had similar grid size. To ensure that the first grid point was placed inside the logarithmic layer, the non-dimensional distance, $y+$, was within the range 10–100 (CHAM, 2000). The convergence criteria ensured that the total normalized residuals, the sum of residuals over the sum of absolute values for all cell volumes and cell faces, are less than a given value (usually, $< 0.5\%$ for airflow and concentration).

Results

Experimental results

For each of the four ventilation systems, the distributions of airflow, temperature, and tracer gas concentration were measured. Because of space limitations, only the concentration results are presented here. Figure 5 shows that the concentration distributions vary significantly among the tested cases because of the different types and placement of supply and exhaust diffusers. In displacement ventilation, the contaminant was displaced to the upper parts of the room by plumes from the internal heat sources or warm walls. Therefore, the concentrations close to the floor were lower than those close to the ceiling. In the upper part of the room, the concentration levels were close to perfect mixing ($c^* = 1$). The location of the sharp

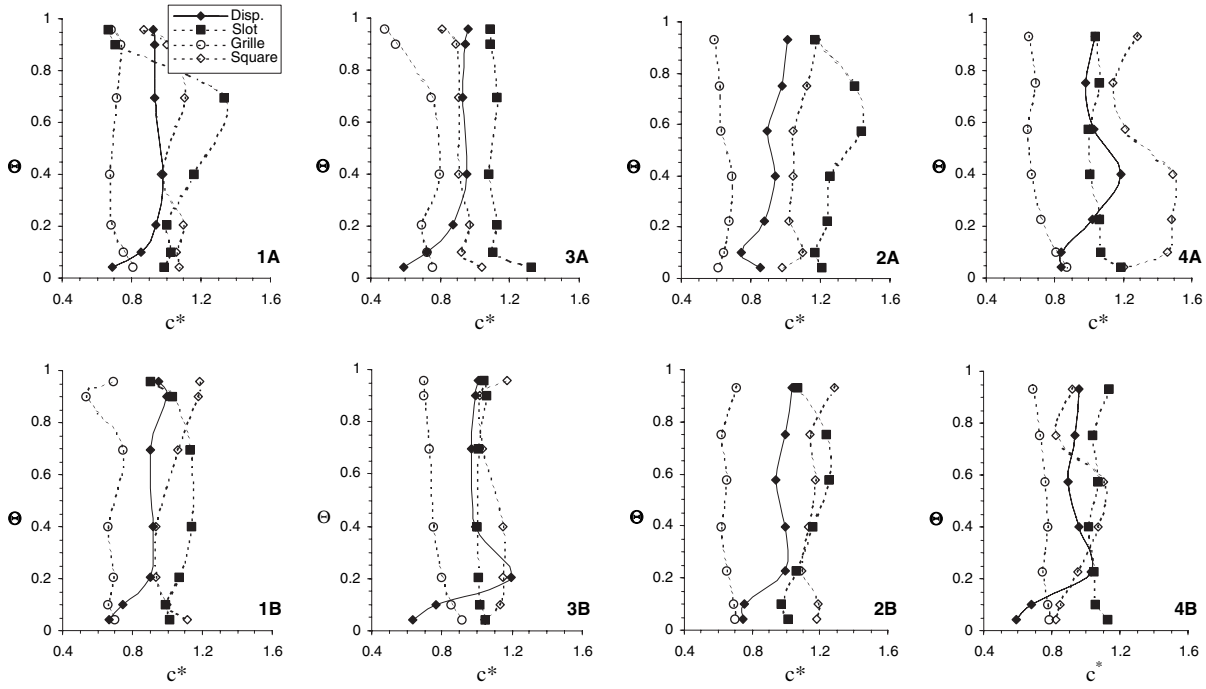

Fig. 5 Measured concentration distributions for four different diffusers. $c^* = (C - C_s)/(C_e - C_s)$, C is the local concentration (mg/m^3), C_s is the supply concentration (mg/m^3), C_e is the exhaust concentration (mg/m^3). $\Theta = Z/H$, Z is the vertical location along the movable poles (m), $H = 2.26$ m is the room height

concentration gradient dividing the room into lower and higher concentration zones is called the stratification height. The location of this stratification layer is important in evaluating the performance of a displacement ventilation system. Based on the data in the present study, the stratification height was at about 0.45 m ($Z/H \sim 0.2$). This stratification height is influenced by both the type and location of the pollutant sources.

It was observed that none of the mixing diffusers reach perfect mixing ($c^* = 1$) in the room. For the four ventilation cases, Table 4 shows dimensionless concentrations c^* at the breathing level of the poles in front of the occupants (occupants 1 and 2), the average values for the breathing plane ($Z = 0.9$ m), and those for the entire occupied zone ($Z = 0$–1.8 m). Overall, the grille diffuser showed higher ventilation effectiveness than the other diffusers. At the occupied zone and the breathing plane (0.2 m below the top surface of the 'seated person'), dimensionless concentrations with the grille diffuser were 20 and 28% lower than those with displacement ventilation, respectively. These lower concentrations with the grill diffuse cannot be attributed to the slightly larger ventilation rate because the concentrations are presented as dimensionless values. The high ventilation effectiveness for the grille diffuser is due to its favorable airflow pattern for this particular contaminant source. The grille diffuser discharges a strong ceiling-attached jet, which drops to the occupied zone near the other side of the room and causes a reverse flow above the floor. The reverse flow transports part of the contaminant directly to the exhaust before the contaminants are dispersed to the higher parts of the room. However, this advantage may disappear for a different exhaust diffuser location or pollutant source height as it will be shown later.

Table 4 Comparison of measured dimensionless concentration c^* at different measuring locations

	Occupant 1 ($Z = 0.9$ m)	Occupant 2 ($Z = 0.9$ m)	Average ($Z = 0.9$ m)	Average (occupied zone $Z = 0$–1.8 m)
Displacement	0.99	1.19	0.96	0.89
Grille	0.66	0.66	0.69	0.71
Slot	1.16	1	1.1	1.1
Square	0.97	1.49	1.09	1.09

Comparison between CFD and experimental data

The extensive validation of the numerical simulation results was performed with all collected data. Figure 6 presents validation for velocity, temperature, and concentration distributions in selected locations with displacement ventilation. Furthermore, Figure 7 shows validation of the concentration distribution for the mixing ventilation with the other three diffusers. Additional figures for comparisons between all of the measured and calculated data are available in the literature (He, 2003).

As shown in Figure 6(a and b), the predicted velocity and temperature profiles match the measurements. The

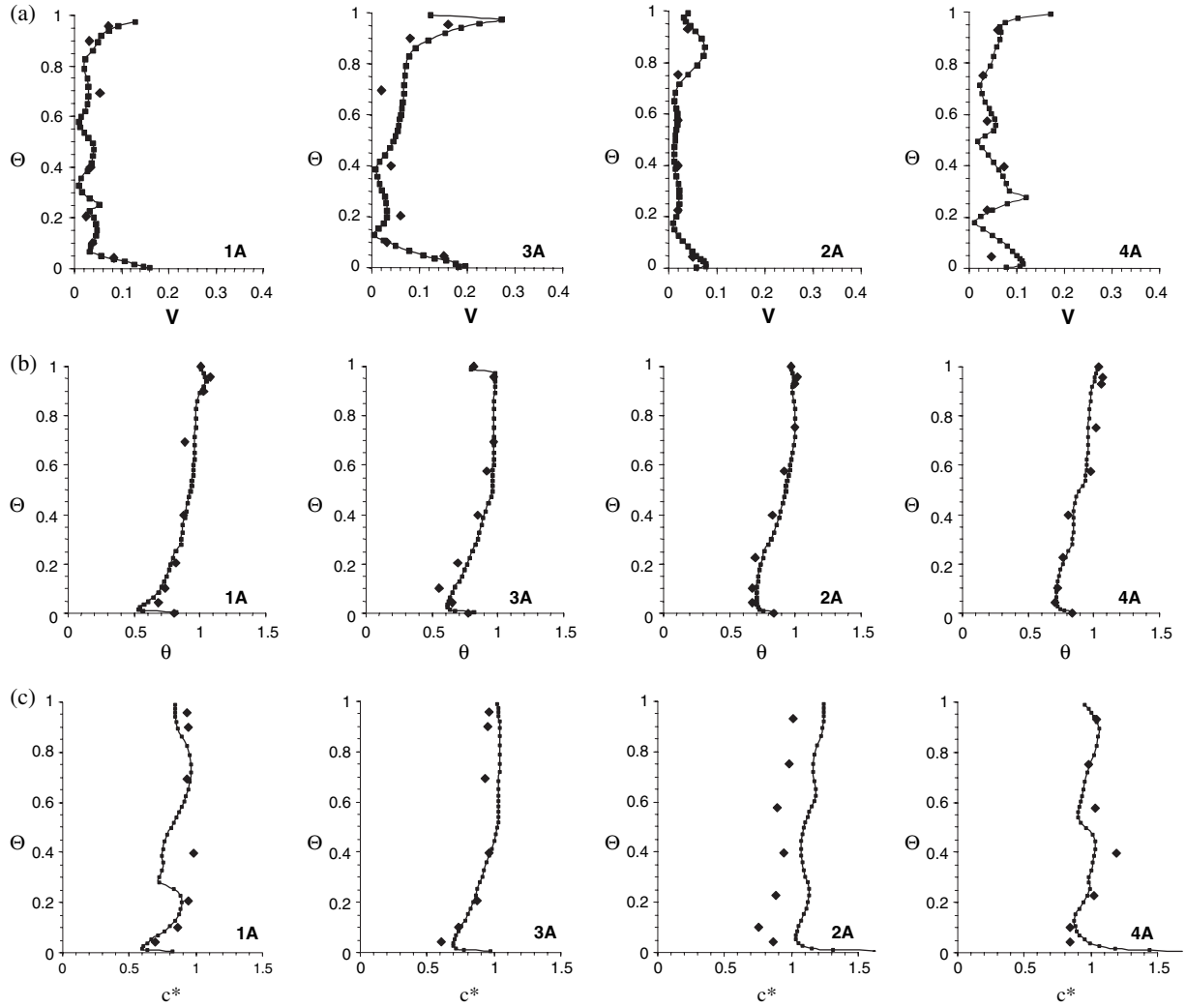

Fig. 6 Comparison of measurements with the calculated data for the displacement ventilation case. $\Theta = Z/H$, Z is the vertical location along the movable poles (m), $H = 2.26$ m is the room height. Symbols: measurement, Lines: computation. (a) Velocity V (m/s); (b) temperature $= (T - T_s)/(T_e - T_s)$, T is the local air temperature, $T_s = 15.9$°C is the supply temperature, $T_e = 24.8$°C is the temperature at room exhaust; (c) tracer gas concentration $c^* = (C - C_s)/(C_e - C_s)$, $C_s = 0.16$ mg/m^3 is the supply concentration, $C_e = 6.16$ mg/m^3 is the concentration at room exhaust

velocity in most of the space is lower than 0.05 m/s. The hot-sphere anemometers may fail to give accurate results in such a low velocity range. For the temperature profiles, there are small temperature differences at pole 3A (room center) ($Z/H = 0.1$–0.4). In this region, the model slightly over-predicts the temperature and under-predicts the velocity. As for the concentration, Figure 6(c) shows that despite discrepancies at a few locations in the room, a qualitative agreement between the model prediction and experimental measurement is established. Both the predicted and measured profiles show a clear stratification with displacement ventilation. Because the pollutant source is lower than the heat sources, the concentration stratification height (at about $Z/H = 0.2$) is lower than the thermal stratification height (at about $Z/H = 0.4$).

Figure 7(a) shows that although the concentration seems to be slightly under-predicted in the grille case, the overall profiles and trends are well predicted. This, together with the agreement between simulated and measured air velocity and temperature (He, 2003), indicates that the CFD model predicts the airflow and pollutant distributions with reasonable accuracy for the grille diffuser ventilation.

Figure 7(b) shows the comparison between the measured and simulated concentrations for the square diffuser. The agreement is very close to the occupant 1 (1A). The under-prediction at the top part of the profile at pole 2A may be caused by a stronger than real jet in the simulation, which makes this calculated local concentration close to the supply air condition. Because the mass balance of contaminants is applied, under-prediction of concentration in the supply jet region (top of 2A) results in the over-prediction of concentration in the exhaust flow region (bottom of 3A). All of these discrepancies between calculated and

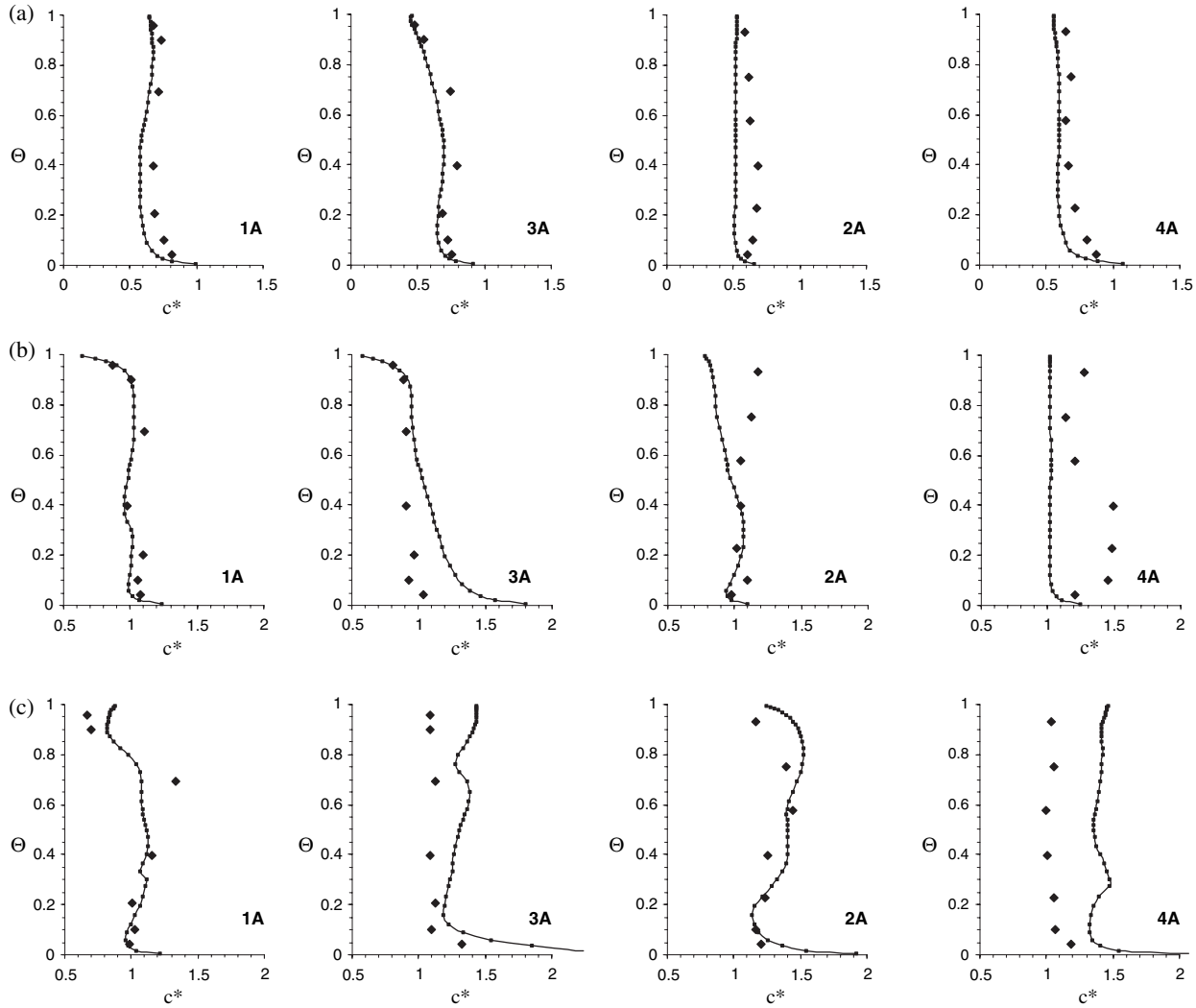

Fig. 7 Comparison of measured concentration distributions with the calculated data; $c^* = (C - C_s)/(C_e - C_s)$, C_s is the supply concentration, C_e is the concentration at room exhaust. $\Theta = Z/H$, Z is the vertical location along the movable poles (m), $H = 2.26$ m is the room height. Symbols: measurement, Lines: computation. (a) Grille diffuser $C_s = 0.16$ mg/m^3, $C_e = 5.16$ mg/m^3; (b) square diffuser $C_s = 0.16$ mg/m^3, $C_e = 6.51$ mg/m^3; (c) slot diffuser $C_s = 0.16$ mg/m^3, $C_e = 6.77$ mg/m^3

measured concentrations are local and on average around 20%. The only area where consistent disagreement is noticed is close to the occupant 2B. This problem is due to complicated local airflow pattern caused by the proximity of the wall attached jet as well as the high density of heat sources (window, occupant and computer). This problem of locally complicated airflow patterns and contaminant distribution is explored in a separate publication because of the complexity of the topic (Srebric et al., 2005).

For the slot diffuser, Figure 7(c) shows that the concentrations are well predicted near the occupant 1 (1A) and pole 2A, but not near the occupant 2 (4A) because of the similar reasons as in the previous case. For both the four-way (square) diffuser and slot diffuser, we found it difficult to model contaminant dispersion with the same accuracy as for the displacement and grill diffusers. The supply jets coming from the slot and four-way diffusers are much more complicated than the ones from the displacement and grille diffusers. The jet complexity is difficult for modeling, so the simulations for slot and four-way diffusers show some discrepancies. In general, the supply diffuser affects the global airflow pattern, leading to deviation in predicted concentration distributions. The following analysis will focus on the displacement and grille diffuser cases as representatives of displacement and mixing ventilation with reliable calculated concentration results.

Effects of airflow and contaminant source location on the contaminant dispersion

The qualitative method is used in the preceding section to validate the CFD simulations with the experimental data. In this section, the airflow pattern

and contaminant source height effects on the contaminant dispersion are further examined by the validated CFD model.

In typical commercial buildings where mechanical ventilation systems are used, the airflow pattern is dominated by the supply diffuser jet and the thermal plumes. In practice, the arrangement of the supply and exhaust diffusers is subject to design freedom and can be very different from space to space. Novoselac and Srebric (2003) demonstrated the importance of the source location relative to the room airflow pattern, which is a direct result of the diffuser layout. In an ideal situation, the contamination source is positioned outside of the main airflow path, outside of the occupied zone and just in front of the exhaust diffuser. In this way, no contaminants would reach the occupants as they are exhausted without any mixing with room air. However, such an ideal situation does not exist in real spaces because source locations and main airflow pattern are difficult to change after the system is installed and in operation. Nevertheless, information on airflow pattern, source location and contaminant distribution is important as it allows assessment of personal exposure and enables understanding of available options for air quality improvements.

The following illustrates the relations between the air quality and the airflow pattern in the displacement and grille cases using the source location analysis. Particularly, the air quality is important in the occupied zone ($Z < 1.8$ m) and the breathing zone ($Z = 1.1$–1.80 m).

In displacement ventilation, the supply air is introduced directly to the occupied zone and the contaminant source is located at the bottom (floor) of the occupied zone. A circulation is formed with a large eddy residing in the occupied zone as shown in Figure 8(a) for the room centerline ($Y = 1.83$ m). A lower portion of the eddy is created by the supply jet, while the upper portion is the reverse flow caused by the pressure differences. While the occupied zone has both supply jet and the reverse flow of the eddy, the breathing zone is completely occupied by the reverse part of this circulation which is behind the source in the circulation flow path. As a result, Figure 8 shows that the concentrations at the breathing zone are nearly the same as that at the exhaust diffuser, whereas the occupied zone is still cleaner than the exhaust air.

To examine the effect of source location on contaminant dispersion in this displacement ventilated room, Figure 9(a, b and c) shows the dimensionless iso-concentration c^* contours when an imaginary area source is elevated to 0.3 m, 1.5 m, and 2.0 m, respectively, with the same source emission rate as that of the floor source. Clearly, as the source is moved to a higher level, the contaminant dispersion paths change accordingly, and, so do the concentrations and stratification

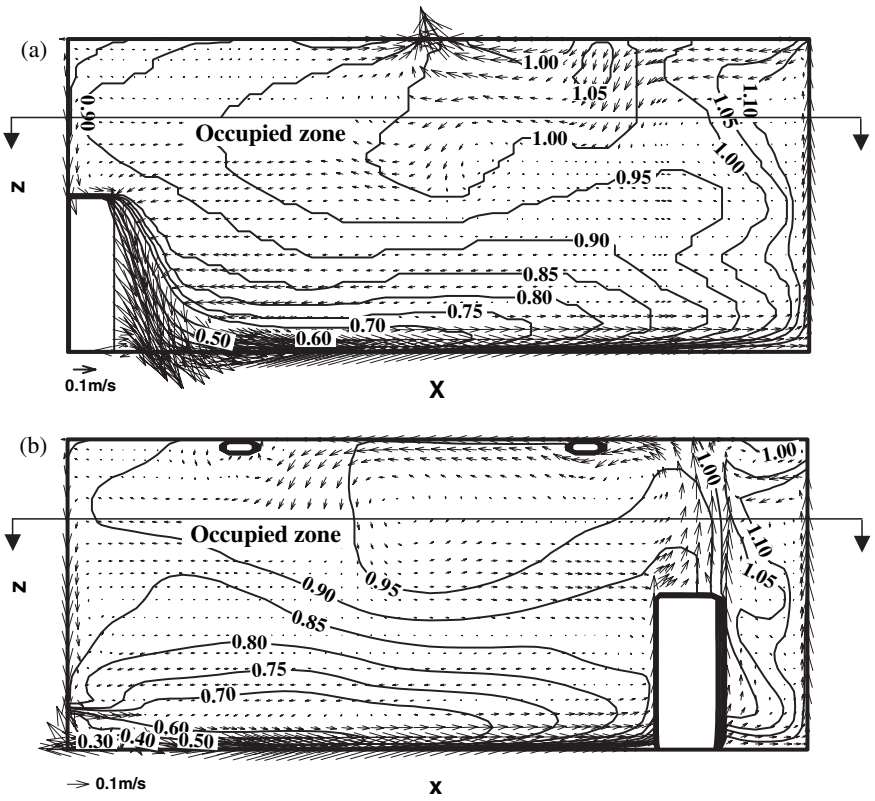

Fig. 8 Dimensionless iso-concentration c* contours and the velocity vector plot at: (a) $Y = 1.83$ m (the room centerline) and (b) $Y = 1.2$ m (person simulator 2b) in displacement ventilation with the exhaust located at the center of the ceiling

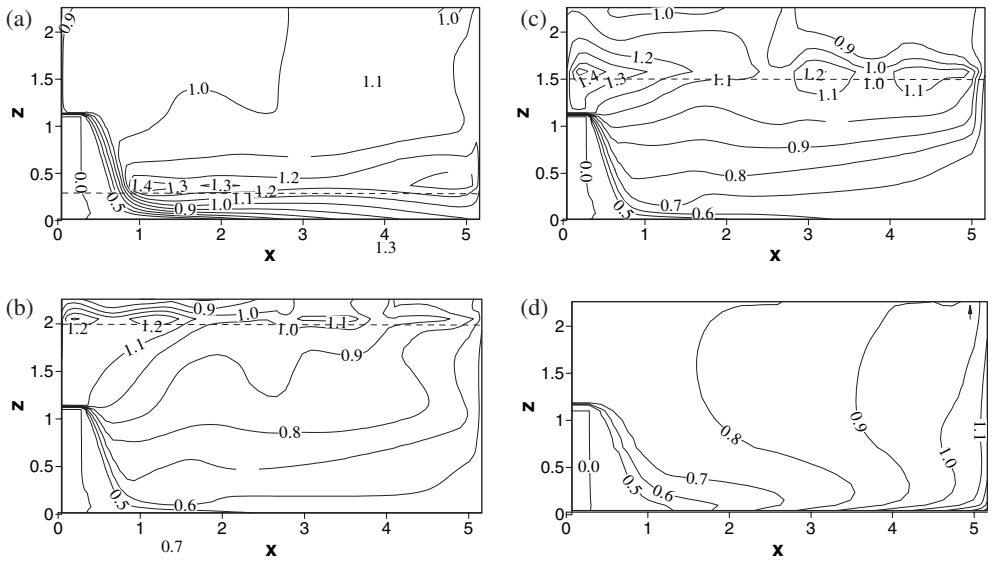

Fig. 9 Dimensionless iso-concentration c^* contours at room centerline ($Y = 1.83$ m) in displacement ventilation with (a) source at $Z = 0.3$ m and exhaust at the ceiling center; (b) source at $Z = 1.5$ m and exhaust at the ceiling center; (c) source at $Z = 2.0$ m and exhaust at the ceiling center; (d) source at floor and exhaust at the other end of the ceiling

heights. When the contaminant source location is only slightly raised (Figure 9a), concentration at the breathing area as well as within the occupied zone becomes higher, indicating that the fresh air attached to the floor is not effectively used to dilute the contaminant. When the source is relocated outside of the occupied zone near the ceiling level (Figure 9c), as expected, direct exhaust occurs and thus lower concentrations at the breathing zone are obtained. Figure 9(d) presents a different distribution pattern when the exhaust is relocated from the ceiling center to the other end of the ceiling. Compared with the original case, considerable improvement of air quality is reached. In this new arrangement, simulation shows that the dominant air circulation in the occupied zone is not changed considerably. However, part of the source is exhausted directly with the window thermal plume before being brought back to the occupied zone with the reverse flow. This transport of the contaminants results in an improved air quality for the large part of the room. This analysis clearly shows how the contaminant stratification is linked to the sources location in respect to the eddy that dominants the airflow pattern. It is also evident that the concentration stratification can occur with an area source in displacement ventilation.

For the studied grille diffuser case, the jet creates a big eddy that circulates through the entire room (see Figure 10). Although small local eddies are observed, they do not exert significant influences on the global contaminant distribution. The strong jets from the supply diffuser intercept the upper boundary of the occupied zone. As a result of non-isothermal jets, the cool air detaches from the ceiling and dilutes the room air contaminants. The reverse flow is located at the lower part of the room and moves directly toward the exhaust diffuser. This flow pattern is favorable for an effective

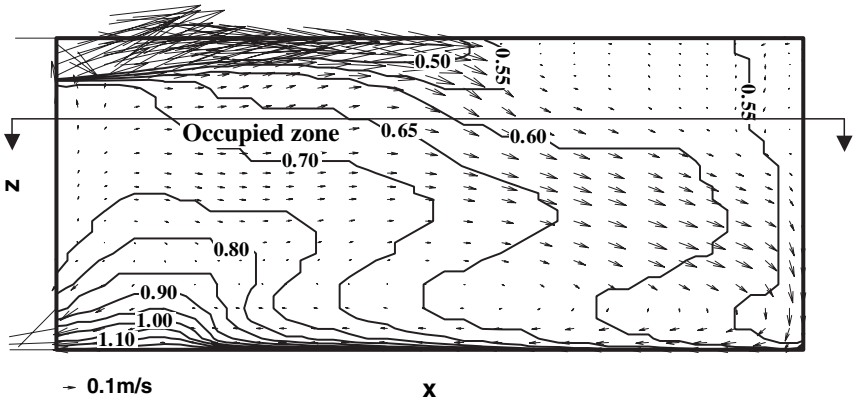

Fig. 10 Dimensionless iso-concentration c^* contours and the velocity vector plot at the room centerline with ventilation by the grille diffuser

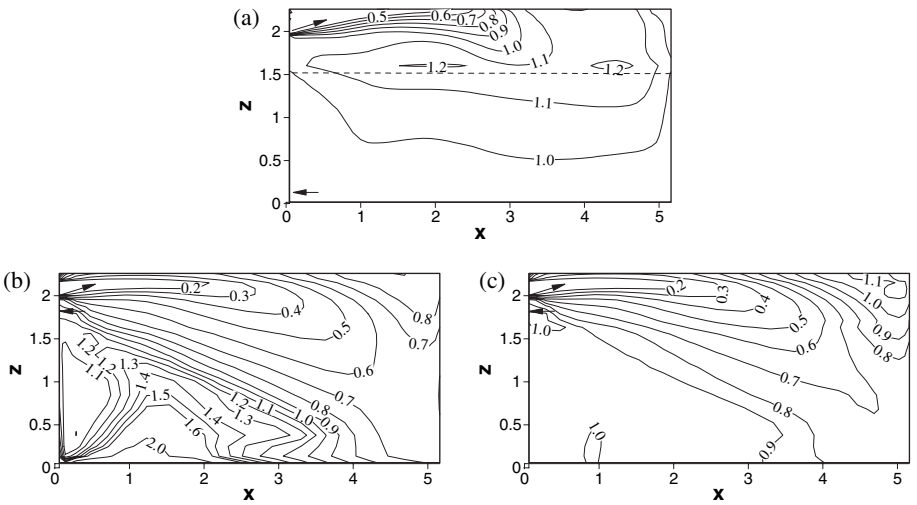

Fig. 11 Dimensionless iso-concentration c^* contours at room centerline ($Y = 1.83$ m) in grill diffuser case with (a) the source at $Z = 1.5$ m; (b) the source at the floor and the exhaust right underneath the supply; (c) the source at $Z = 1.5$ m and the exhaust right underneath the supply

removal of the contaminant because the source is located in front of the exhaust diffuser, resulting in the following airflow path of the main eddy: supply jet → occupied zone → source → exhaust. In most of the region in the room, the concentration is lower than the exhaust concentration. However, if the source is raised to a higher level, the relative positions of the source to the main airflow pattern will be changed. To investigate this effect, three more cases are examined. In the first case, the source is raised to a height of $Z = 1.5$ m. All other conditions remain the same and Figure 11(a) presents the simulation results. The airflow pattern now experiences a circulation with the path: supply jet → source → occupied zone → exhaust. The occupied zone falls behind the source, resulting in higher contaminant concentrations in the occupied zone.

The second modification of the grille diffuser ventilation has a higher position for the exhaust diffuser with a floor level source being the same. The exhaust is re-located to the position right below the supply diffuser, which is typical for grill diffuser installations. In this arrangement, part of the occupied zone is between the source and the exhaust: supply jet → occupied zone/source → occupied zone → exhaust, as it can be seen in Figure 11(b). This arrangement causes a larger part of the occupied zone to be exposed to a concentration higher than the exhaust concentration compared with the original arrangement (Figure 10).

In the third case, the source is elevated to $Z = 1.5$ m and the exhaust diffuser is kept at the higher position. Figure 11(c) shows the dimensionless concentration c^* distribution. Compared with the case in Figure 11(a), the air quality is improved as part of the source is directly transported to the exhaust without entering the occupied zone: supply jet → source → occupied zone/source → exhaust. Based on these simulation results, it can be concluded that the exhaust in the sidewall grille diffuser case should be installed close to the source, or at least at the same level. This conclusion is only valid when grille diffuser is appropriately designed based on its jet throw length. Properly designed sidewall grille diffuser would have a jet attached to the ceiling that would have a sufficient momentum to reach the opposite side wall. In case of inappropriately designed jet or for very low flow rate in off-design conditions, the jet would detach much sooner and drop to the occupied zone causing drafts and different airflow pattern. A second or multiple circulations may appear in the room area far away from the diffuser, where the ventilation effect may be poor and contaminant concentrations high.

Table 5 summarizes the average values of the dimensionless concentration c^* in the breathing zone and the occupied zone for the studied cases. Compared

Table 5 Dimensionless averaged concentration c^* for CFD simulated cases

Case no.	Diffuser	Breathing zone ($Z = 1.1$–1.8 m)	Occupied zone ($Z = 0$–1.8 m)	Description	Figure no.
1-1	Displacement	0.965	0.897	Floor source	8
1-2		0.984	0.994	0.3 m source	9(a)
1-3		1.075	0.903	1.5 m source	9(b)
1-4		0.907	0.789	2.0 m source	9(c)
1-5		0.84	0.81	Exhaust relocated	9(d)
2-1	Grille	0.624	0.658	Floor source	10
2-2		1.07	1.02	1.5 m source	11(a)
2-3		0.96	1.02	Floor source, exhaust relocated	11(b)
2-4		1.11	1.03	1.5 m source exhaust relocated	11(c)

with case 1-1, case 1-5 lowers the concentration by around 10% in the occupied zone and 13% in the breathing zone. This is achieved by simply relocating the exhaust diffuser to a more favorable position with respect to the airflow pattern and source location. Among the four simulated grille cases, only the one with both the source and exhaust at the floor level (case 2-1) has a lower concentration than that of the displacement ventilation. This is a preferred diffuser layout for the contaminant removal from the floor surface. The other grille diffuser cases with relocated source and/or exhaust diffuser show no advantages over the displacement ventilation cases.

The above analyses show that the global airflow pattern and source location have a strong effect on the global distribution of the contaminants. Also, the location of the exhaust diffuser may not greatly affect the airflow pattern or temperature distribution, but can significantly affect the personal exposure levels in the room.

Conclusion

The contaminant dispersion in a ventilated room with an area source release was studied using both experimental measurements and CFD simulations. Different ventilation scenarios were investigated with two types of ventilation: displacement ventilation and three mixing ventilation systems using a grille, square, and slot diffuser, respectively. The simulation results were compared to the experimental data.

In displacement ventilation, the single circulation in the occupied zone propelled by the fresh supply air can dilute the contaminants effectively in the lower level of the room. When the source is at the floor, the circulation restricts the diffusion of the source vertically into the occupied zone. The stratification exists with a lower concentration region at lower level and higher, more uniform concentration at upper level of the room. In the mixing cases studied, the contaminant is found to be nonuniformly distributed in the room and concentrations may be higher or lower compared with a perfect mixing system. In some cases, the higher efficiency of contaminant removal could be reached with proper placement of supply and exhaust diffusers as demonstrated in the grill diffuser case. The global airflow pattern has strong effects on the global distribution of the contaminant. The general exposure level could be estimated through analyzing the relative source positions in the airflow path. The location of the exhaust diffuser may not greatly affect the airflow pattern, but it can significantly affect the exposure level in the room.

Acknowledgements

This research was financially supported by the U.S. National Institute of Occupational Safety and Health (NIOSH) through a SERCA Award (grant no. 1 K01 OH00190) and the National Science Foundation (Grant No. CTS-0134326). We are grateful to Professor Qingyan Chen for his generous support to this study. The experiments were conducted using his full-scale environmental chamber facilities. The authors also greatly benefited from the helpful and constructive comments provided by the reviewers.

References

Brohus, H. (1997) Personal Exposure to Contaminant Sources in Ventilated Rooms, PhD Thesis, Aalborg, Department of Building Technology and Structural Engineering, Aalborg University, ISSN 0902–7953 R9741.

Brohus, H. and Nielsen, P.V. (1996) Personal exposure in displacement ventilated rooms, *Indoor Air*, **6**, 157–167.

CHAM (2000) *PHOENICS Version 3.3*, CHAM Ltd., London, UK.

Chen, Q. and Moser, A. (1991) Simulation of a multiple-nozzle diffuser. In *Proceedings of the 12th AIVC Conference*, Vol. 2, 1–14, Ottawa.

Chen, Q. and Srebric, J. (2002) A procedure for verification, validation, and reporting of indoor environment CFD analyses, *Int. J. HVAC & R Res.*, **8**, 201–216.

Cheong, K.W.D., Djunaedy, E., Poh, T.K., Tham, K.W., Sekhar, S.C., Wong, N.H. and Ullah, M.B. (2003) Measurements and computations of contaminant's distribution in an office environment, *Build. Environ.*, **38**, 135–145.

Fan, Y. (1995) CFD modeling of the air and contaminant distribution in rooms, *Energy Build.*, **23**, 33–39.

Hagström, K., Zhivov, A.M., Siren, K. and Christianson, L.L. (1999) The influence of heat and contaminant source nonuniformity on the performance of three different room air distribution methods, *ASHRAE Trans.*, **105**, 750–758.

Hagström, K., Zhivov, A.M., Siren, K. and Christianson, L. (2002) Influence of the floor-based obstructions on contaminant removal efficiency and effectiveness, *Build. Environ.*, **37**, 55–66.

He, G. (2003) Modeling Indoor Pollutant Exposures under Different Ventilation Schemes, PhD Dissertation, Coral Gables, FL, Department of Civil, Architectural, and Environmental Engineering, University of Miami.

Launder, B.E. and Spalding, D.B. (1974) The numerical computation of turbulent flows, *Comp. Methods Appl. Mech. Energy*, **3**, 269–289.

Nielsen, P.V. (1989) Representation of boundary conditions at supply openings, IEA Annex 20, Research Item 1.11.

Nielsen, P.V. (1997) *The Box Method – A Practical Procedure for Introduction of an Air Terminal Device in CFD Calculation*, Aalborg, Institute for Bygningsteknik, Aalborg Universite.

Novoselac, A. and Srebric, J. (2003) Comparison of air exchange efficiency and contaminant removal effectiveness as IAQ indices, *ASHRAE Trans.*, **109**, 339–349.

Patankar, S.V. (1980) *Numerical Heat Transfer and Fluid Flow*, New York, Hemisphere Publishing Co.

Srebric, J. and Chen, Q. (2002) Simplified numerical models for complex air supply

diffusers, *Int. J. HVAC & R Res.*, **8**, 277–294.
Srebric, J., Hu, B., He, G. and Yang, X. (2005) Critical simulation parameters for accurate CFD predictions of contaminant dispersion from indoor point sources, *Ann. Occup. Hyg.* (in press).
Yang, X. and Chen, Q. (2001) A coupled airflow and source/sink model for simulating indoor VOC exposures, *Indoor Air*, **11**, 257–269.
Yokhot, V., Orzag, S.A., Thangam, S., Gatski, T.B. and Speziale, C.G. (1992) Development of turbulence models for shear flows by a double expansion technique, *Physics Fluids A*, **4**, 1510–1520.
Yuan, X., Chen, Q., Glicksman, L.R., Hu, Y. and Yang, X. (1999) Measurements and computations of room airflow with displacement ventilation, *ASHRAE Trans.*, **105**, 340–352.